International Journal of Mechanical Engineering Research and Technology

ISSN 2454-535X

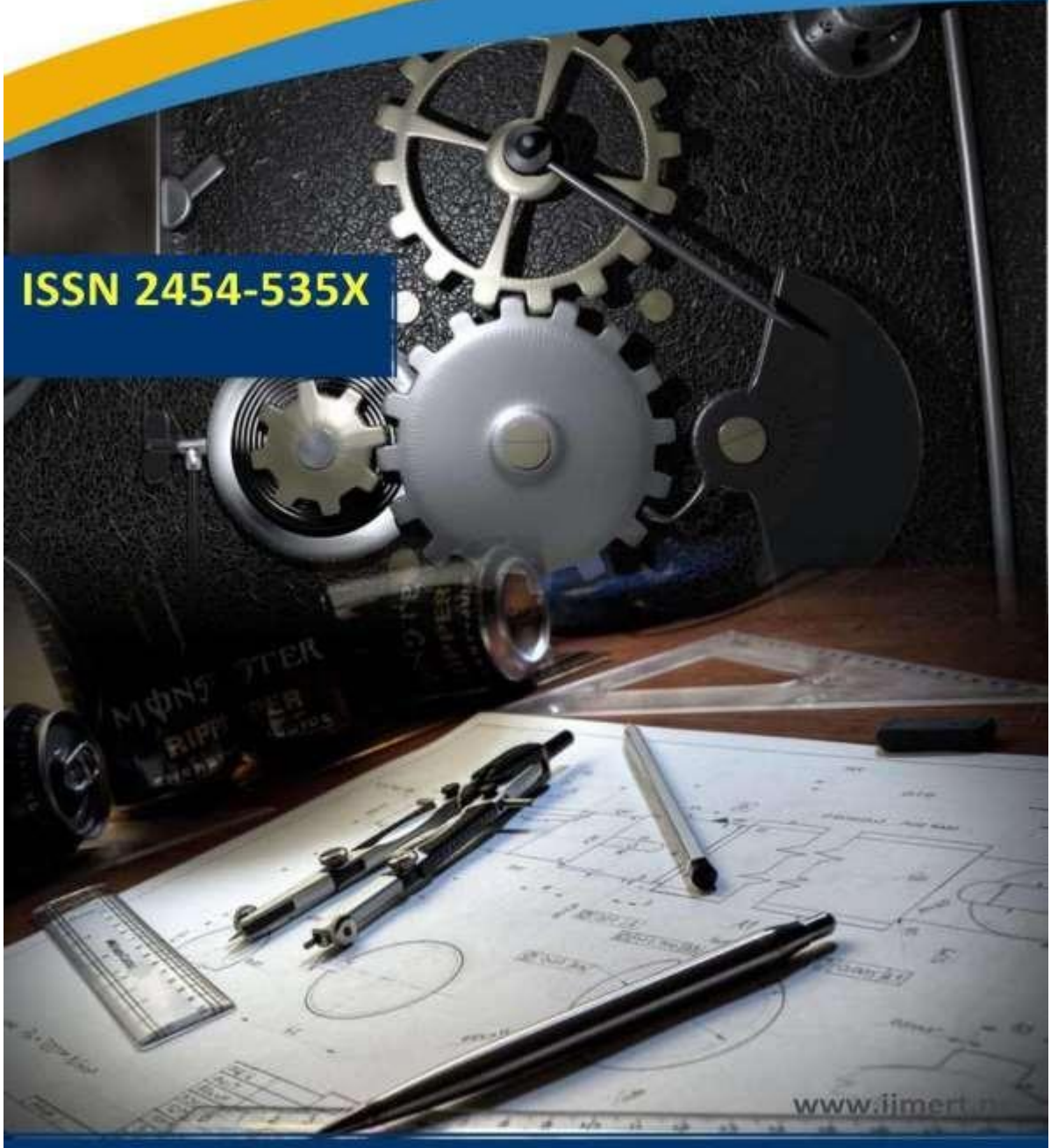

Email ID: info.ijmert@gmail.com or editor@ijmert.net

International Journal of Mechanical Engineering Research and Technology

ISSN 2454 – 535X
www.ijmert.com
Vol. 8 Issue. 1, Jan 2016

Interactions Between Large Solid Particles and HomogeneousShear Turbulence

M. Tokuyama, M. Tanaka, K. Tajiri, H. Nishida & M. Yamakawa

Department of Mechanophysics, Kyoto Institute of Technology, Matsugasaki, Sakyo-Ku, Kyoto 606-8585, Japan

E-mail: sk@kit.ac.jp

ABSTRACT:

Fully resolved simulations of homogeneous shear turbulence laden with a large spherical particle are performed in order to investigate the interaction between a large particle and surrounding turbulent shear flow. We focus on the particles, in zero gravity, whose diameter is about 40 times larger than the Kolmogorov length scale of turbulence with solid-to-fluid density ratios of 1 and 5. An immersed boundary method is adopted to represent the spherical particles. Numerical results show that the turbulence kinetic energy is increased around the particle in the case of the high-density ratio, while it is reduced in the case of the unity density ratio. It is also found that the generation of vortex tubes is activated around the particle in the case of the high-density ratio.

INTRODUCTION

Particle-la den flows are widely encountered in environmental problems and industrial applications such a s sa nd transport in rivers, avalanches, and gas-solid flow in a riser. One of the key factors that affect the dynamics of these flows is the turbulence modulation due to the presence of the dispersed particles [1, 2]. Many studies ha ve been done on turbulence modulation [3-5]. Experimental studies have revealed that both attenuation and augmentation of turbulence occur. Although the particle diameter is a key parameter that determines whether turbulence is augmented or attenuated, the level of turbulence modulation depends on other factors, and the entire picture of turbulence modulation has not yet fully been clarified due to its high complexity. Homogeneous shear turbulence (HST) is one of the simplest flows that have a generation mechanism of turbulence and therefore useful to study the fundamental nature of turbulence modulation. Some two-way coupling simulations were conducted on HST laden with small heavy particles [6, 7]. Recently, fully resolved simulations have been performed for finite-size particles in HST [8, 9]. Tanaka and Teramoto [8] have found that the presence of particles in zero gravity suppresses the growth of turbulence energy of the fluid flow through the enhancement of viscous dissipation. The effect of gravity on turbulence modulation has been investigated in [9]. However, these results were obtained only for relatively small particles that are about 10 times larger than the Kolmogorov length scale.

In the present study, we focus on the situation where the particle diameter is about 40 times larger than the Kolmogorov length scale of turbulence. We examine how the interaction between a large particle and surrounding turbulent shear flow depends on the solid-to-fluid density ratio by fully resolved simulations of HST.

International Journal of Mechanical Engineering Research and Technology

ISSN 2454 – 535X
www.ijmert.com
Vol. 8 Issue. 1, Jan 2016

FORMULATION

Configuration

In the present study, we consider a single solid particle in an incompressible carrier fluid in zero gravity. We consider the motion of the particle in homogeneous turbulence subjected to uniform mean shear, which is in the x_1 direction and is a linear function of x_2

$$\boldsymbol{U} = (\Gamma x_2, 0, 0) \qquad (1)$$

where Γ is the shear rate (see Figure 1). Henceforth, we call the x_1, x_2, and x_3 directions the streamwise, shear, and spanwise directions, respectively. The fluctuating velocity $\boldsymbol{u}'$, which is described by decomposing the velocity field $\boldsymbol{u}$ as $\boldsymbol{u} = \boldsymbol{U} + \boldsymbol{u}'$, is assumed to be homogeneous.331

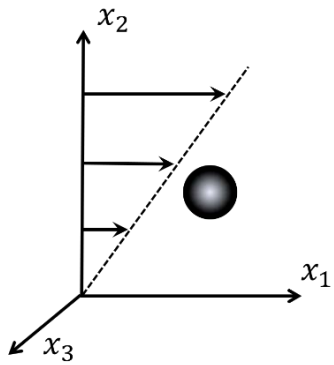

Figure 1. A particle in uniform shear flow.

Governing Equations

The motion of the fluids is described by the Navier-Stokes (NS) equations for incompressible viscous fluids,

$$\frac{\partial \boldsymbol{u}}{\partial t} + (\boldsymbol{u} \cdot \nabla)\,\boldsymbol{u} = -\frac{1}{\rho}\nabla p + \nu \nabla^2 \boldsymbol{u} + \boldsymbol{f} \qquad (2)$$

supplemented with the solenoidal condition $\nabla \cdot \boldsymbol{u} = 0$. Here, $\boldsymbol{u}$, p and ν represent the fluid velocity, pressure, and kinematic viscosity, respectively. The force $\boldsymbol{f}$ is the body force density representing the interactions between the particles and the carrier fluid.

The translational and angular velocities of the particle are described by the Newton-Euler equations,

$$m_p \frac{d\boldsymbol{u}_c}{dt} = -\int_{\Omega_f} \boldsymbol{f}\, dV + \frac{d}{dt}\int_{\Omega_f} \rho_f \boldsymbol{u}\, dV, \qquad (3)$$

International Journal of Mechanical Engineering Research and Technology

ISSN 2454 – 535X
www.ijmert.com
Vol. 8 Issue. 1, Jan 2016

$$I_p \frac{d\boldsymbol{\omega}_c}{dt} = -\rho_f \int_{\Omega} (\boldsymbol{x}-\boldsymbol{x}_c) \times \boldsymbol{f}\, dV + \rho_f \frac{d}{dt} \int_{\Omega} (\boldsymbol{x}-\boldsymbol{x}_c) \times \boldsymbol{u}\, dV, \quad (4)$$

where $m_p = (\pi/6) d_p^3 \rho_p$ and $I_p = m_p d_p^2/10$ are the mass and the moment of inertia of the particle. Here, d_p and ρ_p denote the diameter and density of the particle, respectively. $\boldsymbol{u}_c$, $\boldsymbol{\omega}_c$ and $\boldsymbol{x}_c$ are the velocity, angular velocity and central position of the particle, respectively. Ω denotes the region inside the particle.

Parameters

There are two non-dimensional parameters which characterize single-phase HST; the Taylor-microscale Reynolds number $R_\lambda = \sqrt{5/3}\, \langle u'^2 \rangle / \nu \langle \omega'^2 \rangle^{1/2}$ and the shear rate parameter $S^* = \Gamma \langle u'^2 \rangle / \nu \langle \omega'^2 \rangle$. Here, $\boldsymbol{\omega}' = \nabla \times \boldsymbol{u}'$ is the vorticity fluctuation and $\langle \quad \rangle$ denotes the average over the volume of the computational domain and a time. The Reynolds number based on the shear rate and the dimension of the computational domain in the x_3 direction, $Re_3 = \Gamma L_3^2/\nu$, is an important parameter for statistically stationary HST. The Reynolds number based on the shear rate and the particle diameter, $Re_S = \Gamma d_p^2/\nu$, is one of the dimensionless parameters that characterize the size of the particle.

Computational Method

In this study, our computational method is based on that of Tanaka [9] in which an immersed boundary method [10, 11, 12] was applied to HST laden with solid particles. The Navier-Stokes equations are solved using finite difference schemes on a staggered grid. The second-order central difference scheme is applied in the finite differencing of the convective and viscous terms of the NS equations. They are integrated in time with anexplicit third-order low-storage Runge-Kutta scheme for the convective and viscous terms. In each Runge-Kutta substep, the convection by mean shear is computed at a step separated from that for the residual part of the convective term, using Fourier approximation as in [9].

In the Newton-Euler equations, the volume integrals in the second terms on the right hand sides of the equations are numerically evaluated [11]. The volume fraction of the solid particle in each grid cell, which is required to evaluate the integrals, is expressed by a smoothed Heaviside step function. Lagrangian force points, which are used to evaluate the interaction force $\boldsymbol{f}$, are slightly retracted from the particle surface toward the particle center as in [12]. The multidirect forcing scheme is employed in this study to obtain better approximation of the no-slip/ no- penetration condition on the particle surface [12].

Computational Conditions

Here, we perform simulations for statistically stationary HST to discuss the turbulence modulation around a particle. We carried out preliminary runs at $Re_3 = \Gamma L_3^2/\nu = 2677.3$ (R_λ

International Journal of Mechanical Engineering Research and Technology

ISSN 2454 – 535X
www.ijmert.com
Vol. 8 Issue. 1, Jan 2016

≈ 54), which is close to 2631.9 of Run3 in Pumir [13]. The computational conditions are summarized in Table 1. The influence of the grid resolution was examined for the case of Re_S = 200 and ρ_p/ρ_f = 5.0 using 256×128×128-384×192×192 cubic grid cells. These grid resolutions correspond to $\eta\, k_{max}$ = 3.2 – 4.8, where k_{max} = $\pi/\Delta x$ and η denotes the Kolmogorov length scale in the single-phase HST. It was found that the results obtained with 256×128×128 grid points are in good agreement with those with 384×192×192 grid points. We also carried out runs by changing the solid-to-fluid density ratio as ρ_p/ρ_f = 0.5, 1.0, 2.5, 5.0, 10 to examine its effect on the particle motion and turbulence modulation. It was found that the effect in the case of ρ_p/ρ_f = 0.5 is similar to that in the case of ρ_p/ρ_f = 1.0. It was also found that the influence of the particle monotonically changes with the density ratio for ρ_p/ρ_f > 1.0 (e.g., the particle velocity fluctuations in the streamwise direction increase with the density ratio). Considering these results, we focus on the cases of ρ_p/ρ_f = 1.0 and 5.0 in the present study.

The main runs are conducted in a rectangular computational domain with 4π×2π×2π sides with 384×192×192 cubic grid cells. The computational conditions are summarized in Table 2. The Reynolds number based on the shear rate and the dimension of the computational domain, $Re = \Gamma L^2/\nu$, is set at 4386.5. This Reynolds number is identical to that of Run8 in Pumir [13]. The computational domain is long in the streamwise direction compared with 2π×2π×2π of Run8. The Reynolds number based on the shear rate and the particle diameter, $Re_S = \Gamma d_p^2/\nu$, is set at 200. The ratio of the particle diameter to the grid spacing, $d_p/\Delta x$ = 41.0. The diameter is about 39η. As mentioned above, two cases with different solid-to-fluid density ratios (ρ_p/ρ_f = 1 and 5) considered. For comparison, smaller particles of Re_S = 20 ($d_p/\eta \approx 12$) are considered for the same density ratios. In Table 2, the values in parentheses correspond to the smaller particles. Note that a typical cross-sectional diameter of vortex tubes is about 10η. Statistical quantities are obtained by taking an average over a period in time, more than 2000 in Γt.

Table 1. Computational conditions for preliminary runs

Domain size	4π×2π×2π
Number of grid points	256×128×128 - 384×192×192
Volume fraction	2.55×10^{-3}
Density ratio ρ_p/ρ_f	0.5, 1.0, 2.5, 5.0, 10
Particle diameter $d_p/\Delta x$	35.0-52.5
Shear rate	0.318
Kinematic viscosity	4.69×10^{-3}
$Re = \Gamma L^2/\nu$	2677.3
$Re_S = \Gamma d_p^2/\nu$	200
$\eta\, k_{max}$	3.2-4.8

Table 2. Computational conditions for main runs

International Journal of Mechanical Engineering Research and Technology

ISSN 2454 – 535X
www.ijmert.com
Vol. 8 Issue. 1, Jan 2016

Domain size	$4\pi\times2\pi\times2\pi$
Number of grid points	384×192×192
Volume fraction	2.55×10^{-3} (8.06×10^{-5})
Density ratio ρ_p/ρ_f	1.0, 5.0
Particle diameter $d_p/\Delta x$	41.0 (13.0)
Particle diameter d_p/η	39.1 (12.4)
Shear rate	0.318
Kinematic viscosity	2.86×10^{-3}
$Re = \Gamma L^2/\nu$	4386.5
$Re_S = \Gamma d_p^2/\nu$	200 (20)
ηk_{max}	3.3

RESUTS

Statistical Quantities Averaged over Computational Domain

Turbulence modulation in the whole computational domain is discussed briefly. Statistical quantities including the Taylor-microscale Reynolds number and the shear rate parameter are summarized in Table 3 In the table, ρ_r (= ρ_p/ρ_f) represents the density ratio. In the single-phase turbulence, the Taylor-microscale Reynolds number is 66.0, which is slightly higher than those of 62.6-65.3 obtained for Run8 of Pumir in [13-15]. The shear rate parameter is 7.02 in good agreement with 6.95-7.04 in [14] and 6.99 in [15].

Because of its low volume fraction, HST is modified only slightly due to the presence of the particle. The decrease in the shear rate parameter, which is inversely proportional to the enstrophy, $\langle\omega'^2\rangle/2$, is somewhat noticeable in the case of the large particle with ρ_p/ρ_f = 5. This indicates that the vorticity generation is activated for large particles with high density ratios.

Motion of Particle

Here, we focus on the Lagrangian statistics of solid particles. Table 4 shows the spanwise component of the particle's angular velocity, and particle velocity fluctuations in the streamwise and shear directions. The angular velocity is normalized by that of the mean shear flow $-\Gamma/2$, while the mean-square value of each component of fluctuating particle velocity is normalized by the counterpart of fluctuating fluid velocity. $\langle\ \rangle_t$ denotes the average over a time.

In the case of the small particle of ρ_p/ρ_f = 1, the normalised angular velocity is close to unity. It decreases with an increase of Re_S (or d_p) or solid-to-fluid density ratio.

The mean-square value of the shear component of fluctuating particle velocity is close to that of fluid velocity for the small particle of ρ_p/ρ_f = 1 . It also decreases with an increase of Re_S (or d_p) or solid-to-fluid density ratio. In contrast to the shear component, the mean-square value of the streamwise component of fluctuating particle velocity exceeds that of fluid velocity for the heavy particles. It increases with the particle size for ρ_p/ρ_f = 5. The larger value of the streamwise component was also found in previous studies [16,17].

International Journal of Mechanical Engineering Research and Technology

ISSN 2454 – 535X
www.ijmert.com
Vol. 8 Issue. 1, Jan 2016

Turbulence Modulation around a Particle

We examine the averaged distribution of the quantities on a carrier fluid seen from the center of the particle to clarify the flow structures around the particle. Figure 2 shows the distribution of turbulence kinetic energy (TKE), $\langle u'^2 \rangle/2$, around the large particles. TKE normalized by its average value over the entire computational domain is displayed in the domain of $(8/3)\pi \times (5/3)\pi$. In the case of $\rho_p/\rho_f = 1$, the TKE is reduced around the particle as shown in Figure 2(a). In contrast, the TKE is increased in wide regions on the left and right sides of the particle in the case of $\rho_p/\rho_f = 5$ (see Figure 2(b)).

Table 3. Statistical quantities for fluid flow

	$\langle u_k'^2 \rangle/2$	$\langle \omega_k'^2 \rangle/2$	R_λ	S^*
Single-phase	0.179	2.95	66.0	7.02
Large, ρ_{rr} = 1	0.185	3.06	66.9	6.97
Large, ρ_{rr} = 5	0.182	3.06	65.8	6.87
Small, ρ_{rr} = 1	0.178	2.93	66.0	7.02
Small, ρ_{rr} = 5	0.174	2.87	65.0	7.01

Table 4. Statistical quantities for particles

	$\frac{\langle \omega_{c3}^2 \rangle_t}{(-I'/2)}$	$\frac{\langle u_{c1}'^2 \rangle_t}{\langle u_1'^2 \rangle}$	$\frac{\langle u_{c2}'^2 \rangle_t}{\langle u_2'^2 \rangle}$
Large, ρ_{rr} = 1	0.75	0.73	0.58
Large, ρ_{rr} = 5	0.36	2.40	0.27
Small, ρ_{rr} = 1	0.99	0.95	0.87
Small, ρ_{rr} = 5	0.69	1.04	0.46

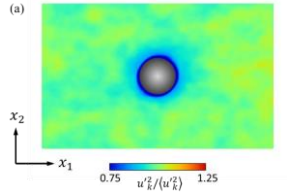

Figure 2. Distribution of turbulence kinetic energy around the large particle. (a) $\rho_p/\rho_f = 1$, (b) $\rho_p/\rho_f = 5$.

International Journal of Mechanical Engineering Research and Technology

ISSN 2454 – 535X
www.ijmert.com
Vol. 8 Issue. 1, Jan 2016

Figure 3 shows the average TKE, Reynolds shear stress and energy dissipation rate as functions of distance from the surface of the particle. The averege over the whole computational domain is used for their normalization. As was shown in Figure 2, the TKE increases (or decreases)

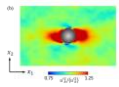

around the large particle with $\rho_p / \rho_f = 5$ (or 1) (see Figure 3(a)). In the case of the small particle, on the other hand, the TKE is reduced around the particle both for the cases of $\rho_p / \rho_f = 1$ and 5. It is seen that the reduction is more remarkable for the higher density ratio of 5. These results indicate that the increase or decrease of TKE (or augmentation or attenuation of turbulence) does not simply depends on the particle diameter.

The normalized Reynolds shear stress is lower than unity near the particle surface (at $r - r_p / \Delta x \approx 3$) in all the cases (see Figure 3(b)). In the region of $r - r_p / \Delta x \geq 10$, the Reynolds shear stress increases (or decreases) around the large particle with $\rho_p / \rho_f = 5$ (or 1). It is interesting that the Reynolds shear stress is significantly reduced around the small particle of $\rho_p / \rho_f = 5$. This indicates that flow structures are significantly modified by the particle of a high density ratio even for small particles.

As is shown in Figure 3(c), the energy dissipation rate is locally enhanced near the surfaces of particles. These regions of high dissipation rate correspond to viscous boundary layers around the particles [8]. The peak values are higher when the particle is larger or the density ratio is higher. It is interesting that the peak value is higher in the case of the small particle with $\rho_p / \rho_f = 5$ than that in the case of the large particle with $\rho_p / \rho_f = 1$.

The flow structures around the particles are examined more in detail. The velocity vectors and the spanwise component of vorticity are shown in Figure 4(a) for the large particle of $\rho_p / \rho_f = 1$. Red regions in the figure indicate that the vorticity component parallel to the mean shear vorticity is large. For the large particle of $\rho_p / \rho_f = 1$, the effect of the particle on the velocity field is confined to a small region around the particle. Correspondingly, the regions of high spanwise vorticity are also confined to the region near the particle surface. The distribution of streamwise vorticity squired, which indicates the activity level of quasi-streamwise vortices, is shown in Figure 4(b) for the large particle of $\rho_p / \rho_f = 1$. In the figure, it is seen that the magnitude of streamwise vorticity is reduced on the left and right sides of the particle, which indicates that the activity level of quasi-streamwise vortices is lowered due to the presence of the particle.

Figure 5 is the same as Figure 4 but for the large particle with $\rho_p / \rho_f = 5$. Compared with the case of $\rho_p / \rho_f = 1$, the presence of the particle influences the flow structures in wider regions around the particle (see Figure 5(a)). The red region of high spanwise vorticity which is generated on the upper (or lower) side of the particle is remarkably extended rightward (or leftward), indicating the occurrence of boundary layer separation. As shown in Figure 5(b), the regions of high streamwise vorticity are extended in the streamwise direction on both sidesof the particle. This indicates that the activity level of quasi-streamwise vortices is higher in these regions.1.21.0

0.8

lence Kinetic

International Journal of Mechanical Engineering Research and Technology
ISSN 2454 – 535X
www.ijmert.com
Vol. 8 Issue. 1, Jan 2016

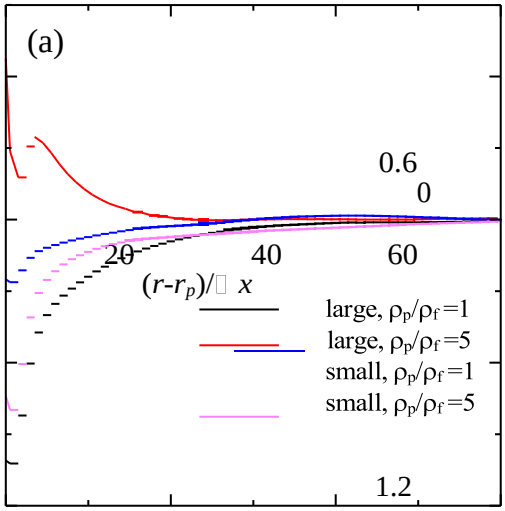

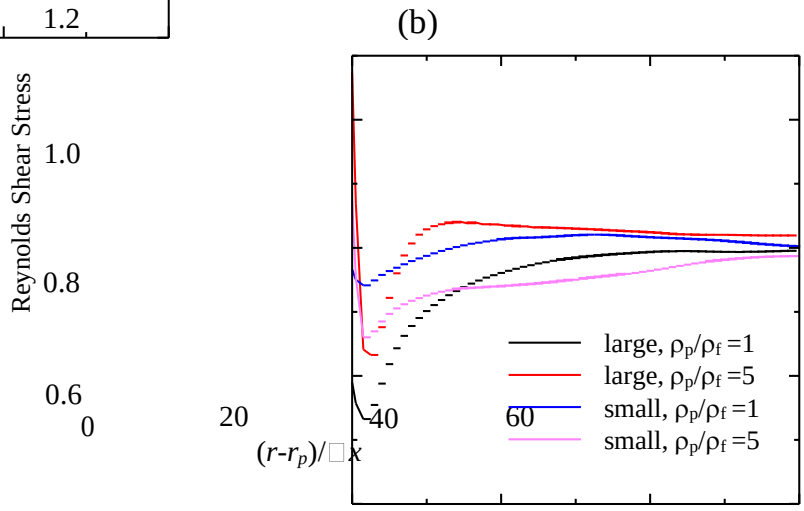

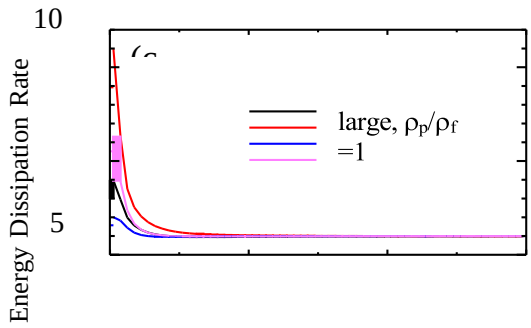

International Journal of Mechanical Engineering Research and Technology

ISSN 2454 – 535X
www.ijmert.com
Vol. 8 Issue. 1, Jan 2016

Figure 3. (a) Turbulence kinetic energy, (b) Reynolds shear stress, (c) viscous dissipation rate around the particle.

In Figure 6, vortex tubes and vortex layers are shown for the large particles. They are respectively visualized by the isosurfaces of $\lambda 2/\Gamma^2 = -8$ [18] and $\Phi A_{ij}\Phi_+/\Gamma^2 = 14$, where $\Phi A_{ij}\Phi_+$ represents the largest eigenvalue of the tensor $A_{ij} = S_{ik}\,\Omega_{kj} + S_{jk}\,\Omega_{ki}$, and S_{ij} and Ω_{ij} denote the rate-of strain and vorticity tensors, respectively [19]. As shown in Figure 6(b), a large separated vortex layer is seen on the right side of the particle with $\rho_p/\rho_f = 5$. In fact, the leftward slip velocity of the particle is quite high at this moment, which is consistent with the large particle velocity fluctuations in the streamwise direction (see Table 4). The vortex layers thus detached from the particle roll up into vortex tubes, leading to the generation of quasi-strea mwise vortices. This further leads to the increase in the TKE as shown in Figure 2(b).

The results obtained in this paper indicate that whether TKE is increased or decreased around the particle is not simply determined by the particle diameter. It is interesting to know whether the turbulence modulation depends on a different single parameter such as the Reynolds number based on the slip velocity or depends on multiple parameters in a complex way. Further studies are needed to answer this intricate question.

CONCLUSIONS

Fully resolved simulations of homogeneous shear turbulence laden with a single large particle are performed in order to deepen the understanding of the turbulence modulation due to the presence of solid particles. We focus on the particles whose diameter is about 40 times larger than the Kolmogorov length scale of turbulence with solid- to-fluid density ratios of 1 and 5 in zero gravity. Smaller particles of about 12η are also considered for comparison. It is found that the turbulence kinetic energy is increased around the large particle with $\rho_p/\rho_f = 5$, whereas it is

reduced in the other cases including that of the large particle with $\rho_p/\rho_f = 1$. It is also found that the genera t ion of quasi-streamwise vortices is activated around the particle in the case of the large particle with the high density ratio.

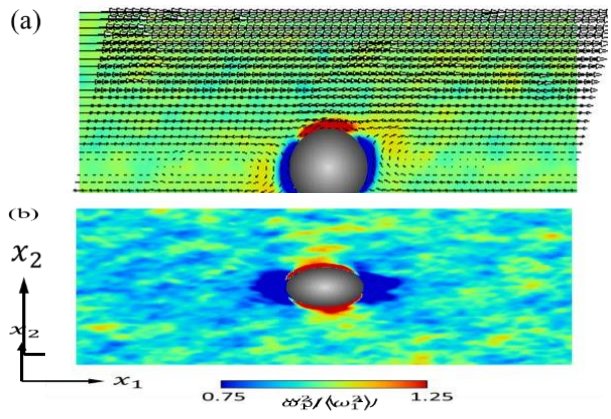

International Journal of Mechanical Engineering Research and Technology

ISSN 2454 – 535X
www.ijmert.com
Vol. 8 Issue. 1, Jan 2016

Figure 4. (a) Velocity field and spanwise component of vorticity, and (b) streamwise vorticity squired around thelarge particle with $\rho_p / \rho_f = 1$.

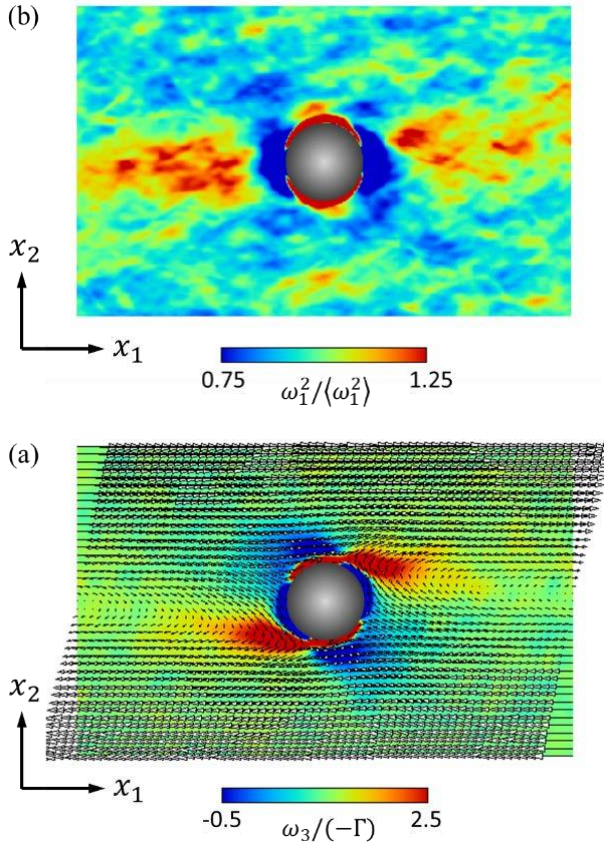

International Journal of Mechanical Engineering Research and Technology

ISSN 2454 – 535X
www.ijmert.com
Vol. 8 Issue. 1, Jan 2016

Figure 5. The same as Figure 4 but for $\rho_p / \rho_f = 5$.

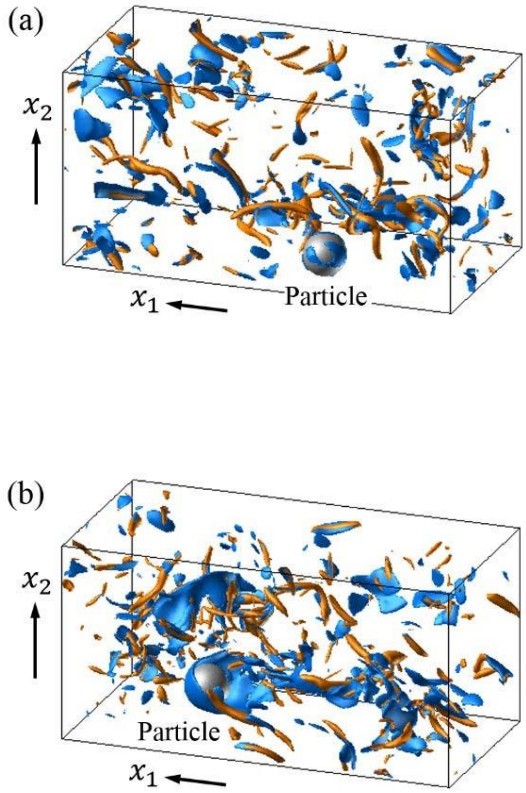

Figure 6. Vortex tubes (orange) and layers (blue) in HST laden with a large particle. (a) $\rho_p / \rho_f = 1$, (b) $\rho_p / \rho_f = 5$. NOMENCLATURE

$\Vert A_{ij} \Vert$ the largest eigenvalue of $A_{ij} = S_{ik}\ \Omega_{kj} + S_{jk}\ \Omega_{ki}$.
d_p particle diameter
$\boldsymbol{f}$ interaction force
I_p moment of inertia
k_{max} maximum wavenumber
m_p mass of the particle
p pressure
r distance from the particle center
r_p particle radius

International Journal of Mechanical Engineering Research and Technology
ISSN 2454 – 535X
www.ijmert.com
Vol. 8 Issue. 1, Jan 2016

Re Reynolds number based on the computational domain *Re*S Re number based on shear rate and bubble diameter $R\lambda$ Taylor-microscale Reynolds number
S^* shear rate parameter
Sij ra te-of-strain tensor
t tim e
u fluid velocity
u' fluid velocity fluctuations
uc particle velocity
U mean shear velocity
V volume
x position
xc position of the particle center
Δx grid spacing
Γ shear ra te
η Kolmogorov length scale of turbulence
v kinema tic viscosity
 density
 r solid-to fluid density ratio
$\boldsymbol{\omega}$ vorticity
$\boldsymbol{\omega}'$ vorticity fluctuations
$\boldsymbol{\omega}_C$ angular velocity of particle
Ω inner region of the particleΩ_{ij} vorticity tensor *Subscripts*
f carrier fluidp particle

REFERENCES

[1] C.T. Crowe, J.D. Schwarzkopf, M. Sommerfeld, Y. Tsuji. *Multiphase Flows with Droplets and Particles*. 2nd ed. Boca Raton: CRC Press, 2011.

[2] S. Balachandar, J.K. Eaton. "Turbulent dispersed multiphase flow". *Annual Review of Fluid Mechanics*, Vol. 42, pp. 111-133, 2010.

[3] Y. Tsuji, Y. Morikawa. "LDV Measurements of an air-solid two-phase flow in a horizontal pipe". *Journal of Fluid Mechanics*, vol. 120, pp. 385-409, 1982.

[4] K.D. Squires, J.K. Eaton. "Particle response and turbulence modification in isotropic turbulence". *Physicsof Fluids A*, Vol. 2, pp. 1191-1203, 1990.

[5] F. Picano, W.P. Breugem, L. Brandt. "Turbulent channel flow of dense suspensions of neutrally-buoyant spheres". *Journal of Fluid Mechanics*, Vol. 764, pp. 463-487, 2015.

[6] F. Mashayek. "Droplet-turbulence interactions in low-Machnumber homogeneous shear two-phase flows". *Journal of Fluid Mechanics*, Vol. 367, pp. 163-203, 1998.

International Journal of Mechanical Engineering Research and Technology

ISSN 2454 – 535X
www.ijmert.com
Vol. 8 Issue. 1, Jan 2016

[7] A.M. Ahmed, S. Elghobashi. "On the mechanisms of modifying the structure of turbulent homogeneous shear flows by disperse particles". *Physics of Fluids*, Vol. 12, pp. 2906-2930, 2000.

[8] M. Tanaka, D. Teramoto. "Modulation of homogeneous shear turbulence laden with finite-size particles". *Journal of Turbulence*, Vol. 16, pp. 979-1010, 2015.

[9] M. Tanaka. "Effect of gravity on the development of homogeneous shear turbulence laden with finite-size particles". *Journal of Turbulence*, Vol. 19, pp. 1144-1179, 2017.

[10] M. Uhlmann. "An immersed boundary method with direct forcing for the simulation of particulate flows". *Journal of Computational Physics*, Vol. 209, pp. 448-476, 2005.

[11] T. Kempe, J. Fröhlich. "An improved immersed boundary method with direct forcing for the simulation ofparticle la den flows". *Journal of Computational Physics*, Vol. 231, pp. 3663-3684, 2012.

[12] W.P. Breugem. "A second-order accurate immersed boundary method for fully resolved simulations of particle-la den flows". *Journal of Computational Physics*, Vol. 231, pp. 4469-4498, 2012.

[13] A. Pumir. "Turbulence in homogeneous shear flows". *Physics of Fluids*, Vol. 8, pp. 3112-3127, 1996.

[14] M. Tanaka. "Inverse transverse migration of small bubbles in turbulence". *Journal of the Physical Societyof Japan*, Vol. 82, 044401, 2013.

[15] M. Tanaka. "Motion of spherical bubbles in homogeneous shear turbulence". *Fluid Dynamics Research*, Vol. 51, 035505, 2019.

[16] M.W. Reeks. "On the constitutive relations for dispersed particles in nonuniform flows. I. Dispersion in a simple shear flow". *Phys Fluids A*, Vol. 5, pp. 750-761, 1993.

[17] L.M. Liljegren. "The effect of a mean fluid velocity gradient on the streamwise velocity variance of a particle suspended in a turbulent flow". *International Journal of Multiphase Flow*, Vol. 19, pp. 471-484, 1993.

[18] J. Jeong, F. Hussa in. "On the identification of a vortex". *Journal of Fluid Mechanics*, Vol. 285, pp. 69-94, 1995.

[19] K. Horiuti, Y. Takagi. "Identification method for vortex sheet structures in turbulent flows". *Physics of Fluids*, Vol. 17, 121703, 2005.